JOURNAL OF GEOPHYSICAL RESEARCH, VOL. 101, NO. D10, PAGES 15,033–15,049, JUNE 27, 1996

# Modulation of equatorial subseasonal convective episodes by tropical-extratropical interaction in the Indian and Pacific Ocean regions

Gerald A. Meehl,[1] George N. Kiladis,[2] Klaus M. Weickmann,[3] Matthew Wheeler,[2,4] David S. Gutzler,[5] and Gilbert P. Compo[4]

**Abstract.** Composite relationships among outgoing longwave radiation, sea level pressure, surface winds, and upper tropospheric circulation are examined for northern winter during subseasonal episodes of eastward progression of convection from the Indian Ocean to the western Pacific. This evolution often culminates with westerly wind burst events and strong air-sea interaction associated with regional-scale convective blowups in the western equatorial Pacific. We first document some of these interactions in the composites for two timescales, the submonthly (6–30 days) and that of the Madden-Julian Oscillation (MJO) timescale (30–70 days). We then analyze the December 1992 period during the Tropical Ocean Global Atmosphere Coupled Ocean-Atmosphere Response Experiment (TOGA COARE) to illustrate how these composite relationships are manifested in a case study. Convection in the Indian Ocean for the composites is shown to be associated with a northern hemisphere wave train at 200 mbar, arcing through the midlatitudes, that can contribute to convective blowups farther east on the submonthly (6–30 days) timescale in the Intertropical Convergence Zone (ITCZ) in the eastern Pacific. The eastern Asian trough that is part of this wave train is associated with pressure surges from the northern hemisphere and subsequent convection over Southeast Asia. As the MJO convective envelope moves east to Australasia, midlatitude wave trains in either hemisphere include upper level troughs east of Asia and Australia and pressure surges from either hemisphere that contribute to pressure rises over the Indonesian region and a subsequent shift of the convective envelope to the western Pacific. The vertical wind structure for the December 1992 case study is consistent with the composite surface and upper level winds and also shows strong vertical wind shear in the boundary layer, a sharply defined westerly maximum near 700 mbar and an intensification of the upper level easterlies near 100 mbar. Very deep westerlies (to 200 mbar) are confined to shorter timescales. The case study illustrates the various time and space scale interactions noted in the composites. Reciprocal interactions between the tropics and the midlatitudes on the submonthly and MJO timescales in both the composites and the case study involve pressure surges and wave interaction that influence subsequent convection as the convective envelope migrates eastward from the tropical Indian to Pacific Ocean region.

## 1. Introduction

An earlier study [*Kiladis et al.*, 1994] documented large-scale aspects of westerly wind burst events in the western equatorial Pacific, confirming previous work [e.g., *Chu*, 1988] that showed pressure surges from Asia being important at times in initiating near-equatorial pressure gradients, surface convergence, a blowup of deep convection, and westerly winds at the surface. *Kiladis et al.* [1994] also described a composite evolution of these features through the use of cross correlations between outgoing longwave radiation (OLR) and global circulation analyses. Events on two separate timescales were identified during the evolution of westerly wind events, the "submonthly" or 6- to 30-day timescale and the Madden-Julian Oscillation (MJO) or 30- to 70-day timescale [see *Madden and Julian*, 1994]. A similar timescale to the submonthly one shown here has also been examined by *Murakami* [1980], *Lyons* [1981], *Hartmann et al.* [1992], *Schrage and Vincent*, 1995], and *Chen et al.* [1995]. Some of the features examined here were present during a westerly wind burst event in November 1989 studied in detail by *McPhaden et al.* [1992] and *Kiladis et al.* [1994].

Previous studies have suggested important interactions between tropics and midlatitudes that can affect energy dispersion from regional-scale convection in the tropics and subsequent downstream (eastward) development [e.g., *Lau et al.*, 1983; *Lau and Chang*, 1987; *Ferranti et al.*, 1990; *Hoskins and Ambrizzi*, 1993]. *Hsu et al.* [1990] postulated that tropical convection could set up conditions in the extratropics that contribute to subsequent tropical convection to the east. There are also considerable time and space scale interactions within the tropics that play a role in the eastward movement of convec-

[1]National Center for Atmospheric Research, Boulder, Colorado.
[2]Aeronomy Laboratory, NOAA, Boulder, Colorado.
[3]Climate Diagnostics Center, Boulder, Colorado.
[4]Program in Atmospheric and Oceanic Sciences, University of Colorado, Boulder.
[5]University of New Mexico, Albuquerque.



Paper number 96JD01014.
0148-0227/96/96JD-01014$09.00

tion from the Indian to Pacific sectors on the subseasonal timescale [e.g., *Lau et al.*, 1989; *Weickmann and Khalsa*, 1990; *Hendon and Liebmann*, 1994] as well as on the interannual timescale [*Meehl*, 1994]. Some of the features associated with the eastward progression of convection from the tropical Indian to Pacific Ocean regions have been shown to influence the Australian monsoon [*Davidson et al.*, 1983], and characteristics of cold surges from the southern hemisphere have been documented for the Australian sector [*Love*, 1985].

In this paper we will examine interactions and processes taking place at the submonthly and MJO timescales, extend the *Kiladis et al.* [1994] work to larger spatial scales associated with the two timescales, and expand on some of the concepts of the *Hsu et al.* [1990] study to document additional characteristics associated with tropical-midlatitude interaction and subseasonal convective events in the tropical Indian and western Pacific. We will address these issues by first identifying composite features involved with the eastward progression of regional-scale convection along the equator from the Indian to Pacific Ocean regions in the context of tropical-midlatitude interaction and downstream development. We will then analyze a case study taken from the Tropical Ocean Global Atmosphere Coupled Ocean-Atmosphere Response Experiment (TOGA COARE) period [*Webster and Lukas*, 1992] during December 1992. In the case study, we will look for evidence of processes noted in the composites that take place during this eastward progression of convection. We will conclude by postulating a scenario for the eastward shift of convection involving the various time and space scale interactions discussed in the paper. This scenario will provide a framework for subsequent studies, some currently under way, intended to quantify some of the details of the relationships presented in this paper.

## 2. Data and Methodology

As shown in the work of *Kiladis et al.* [1994], we make use of the National Meteorological Center (NMC) operational analyses as well as the European Centre for Medium-Range Weather Forecasts (ECMWF) operational analyses. The two analysis products are qualitatively comparable for the present application [*Trenberth and Olson*, 1988]. The cross-correlation technique utilized here is the same as that used by *Kiladis et al.* [1994] and involves filtered OLR averages over a specified base region being regressed against identically filtered wind, 200 mbar streamfunction, and sea level pressure (SLP) data for the northern winters of 1985–1986 through 1992–1993. Initially, the first three harmonics of the annual cycle are subtracted from the time series at each grid point to obtain daily perturbations of all variables. Then a Lanczos digital filter is applied to separate the fluctuations into two frequency bands: 30–70 days (the timescale of the MJO) and the submonthly timescale of 6–30 days. This filter utilizes 121 weights of daily data, resulting in a very sharp response at the cutoff frequency [see *Kiladis and Weickmann*, 1992a]. A time series of filtered OLR over a specified area is then regressed against filtered wind, pressure, and streamfunction data at all other global grid points. As noted by *Kiladis et al.* [1994], a canonical or "composite" circulation anomaly associated with a given OLR anomaly is obtained along with significance of the linear relationship between convection and circulation. Field significance has also been calculated [*Livezey and Chen*, 1983], and all fields shown here are significant at better than the 95% confidence limit.

## 3. Composite Results From Cross Correlations

### Indian Ocean

We begin the examination of composite submonthly timescale convection and associated atmospheric circulation in the Indian Ocean region. This base area as well as the others in the Southeast Asian and western Pacific regions are chosen as representative of stages in the eastward progression of convection to illustrate the various time and space scale interactions. Figure 1 shows the cross correlations between 6- to 30-day OLR in a base area in the eastern Indian Ocean (90°E-100°E, 5°S-5°N) and 200 mbar streamfunction at all other grid points. A comparable plot for 200 mbar streamfunction anomalies at day 0 and day +4 is shown by *Kiladis and Weickmann* [1992a, Figure 9].

At day −2 (Figure 1a) there is a weak wave train arcing downstream into the northern hemisphere across the North Pacific to North America and an anticyclonic center over India associated with previous convective activity on this timescale south of India. At day 0 (Figure 1b), the peak of convection in the eastern Indian Ocean base area, the anticyclone has moved eastward over Bangladesh with a cyclonic circulation centered south of Korea and a wave train extending across the North Pacific with positively tilted waves (i.e., exhibiting a positive correlation between zonal and meridional wind anomalies) propagating into low latitudes over the eastern Pacific. The trough over Korea will be shown below to be related to midlatitude pressure surges that contribute to the initiation of convection in the tropical western Pacific.

By day +2 (Figure 1c) the downstream northern hemisphere wavetrain noted in Figure 1b is well developed, with a weaker wave train in the southern hemisphere. The waveguide corresponding to this wave train has been identified by *Hoskins and Ambrizzi* [1993] and is related to the presence of the Asian jet and upper level westerly flow at low latitudes over the eastern Pacific. Enhanced convection is occurring in the Intertropical Convergence Zone (ITCZ) region in the eastern Pacific near 150°W in association with upward motion ahead of the trough near the ITCZ. *Kiladis and Weickmann* [1992b] show that this is a typical pattern during eastern Pacific submonthly convective events during northern winter and spring.

It has been noted [*Kiladis and Wheeler*, 1995; *Numaguti*, 1995] that such vorticity intrusions into the tropics of the eastern Pacific can be associated with the formation of anomalous 850 mbar cyclonic circulation with spatial and temporal characteristics that resemble the $n = 1$ equatorial Rossby wave of *Matsuno* [1966]. These disturbances propagate westward at about 8 m $s^{-1}$ and are subsequently associated with anomalous convection in the western Pacific [see *Kiladis et al.*, 1994, Figure 6]. Thus as is discussed below, there is a likelihood of at least three mechanisms by which connections to the east from Indian Ocean convection could contribute to convection in the western equatorial Pacific. The first mechanism involves the slow eastward propagation of the MJO itself [e.g., *Madden and Julian*, 1994]. The second mechanism is through the forcing of midlatitude wave trains with troughs over eastern Asia or eastern Australia conducive to midlatitude pressure surges over Southeast Asia and the western Pacific that contribute to the initiation of convection [e.g., *Compo et al.*, 1995]. Such convective episodes have also been shown to initiate eastward moving equatorial Kelvin wavelike phenomena that could affect convection to the east [e.g., *Weickmann and Khalsa*, 1990]. The third mechanism involves westward propagating cyclone

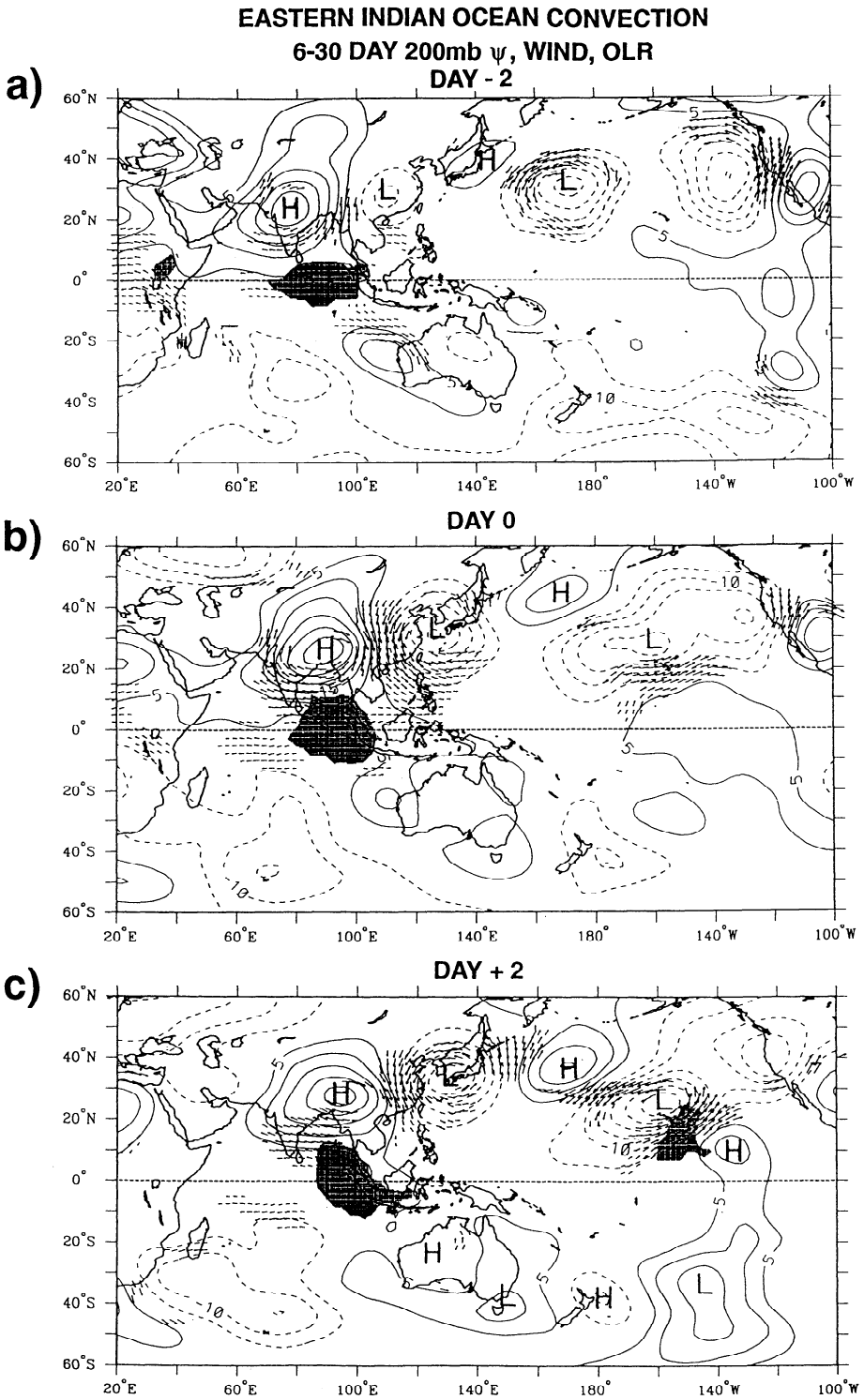


**Figure 1.** Composite outgoing longwave radiation (OLR), 200 mbar streamfunction and 200 mbar vector wind anomalies in the 6- to 30-day band (submonthly timescale) computed for the period December-February 1985-1986 through 1992-1993 associated with area-averaged OLR in a base region in the eastern Indian Ocean (5°S-5°N, 90°E-100°E, indicated by box outline in plots): (a) circulation leading the peak in convection (as represented by low OLR in the base region) by two days (day −2); (b) simultaneous relationship (day 0); (c) two days after the peak in convection (day +2). OLR standard deviation is 17.2 W $m^{-2}$. Contour interval is $5 \times 10^5$ $m^2$ $s^{-1}$. Only locally statistically significant wind vectors are shown. Negative OLR anomalies (indicative of enhanced convection) less than −10 W $m^{-2}$ are shaded.

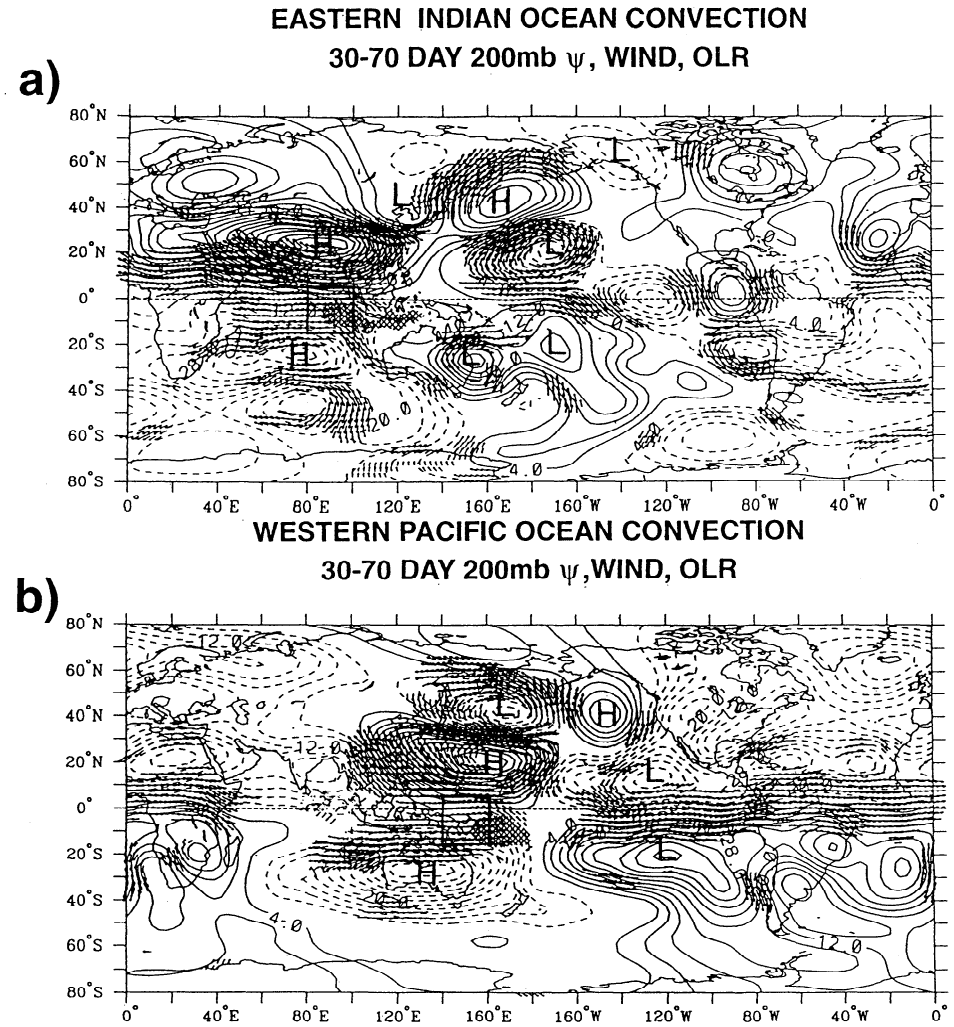


**Figure 2.** Composite OLR, 200 mbar streamfunction and 200 mbar vector wind anomalies in the 30- to 70-day band (Madden-Julian Oscillation (MJO) timescale) computed for the period December-February 1985-1986 through 1992-1993: (a) circulation associated with area-averaged OLR in a base region in the eastern Indian Ocean (15°S-5°N, 80°E-100°E, indicated by box outline in plot); (b) circulation associated with area-averaged OLR in a base region in the western equatorial Pacific Ocean (15°S-5°N, 140°E-160°E, indicated by box outline in plot). Circulation is shown six days following the peak in area-averaged OLR in the base area.

pairs with the structure of equatorial Rossby waves. These are linked to vorticity intrusions into the tropics of the eastern Pacific associated with upper level midlatitude Rossby wave activity that is connected to tropical east Indian Ocean convection.

To examine the midlatitude wave train connection to intraseasonal convection in the Indian Ocean, the cross correlations of 30- to 70-day filtered OLR in the base area 80°E-100°E, 15°S-5°N with 200 mbar streamfunction at all other grid points are shown in Figure 2a (this base area is somewhat larger than the base area in Figure 1 due to the larger spatial scales of the 30- to 70-day filtered OLR). This represents primarily the perturbation of the atmospheric circulation associated with convection in the Indian Ocean region of Figure 1 on the MJO timescale [e.g., see *Kiladis and Weickmann*, 1992a]. A downstream ridge-trough pattern which is similar in some respects to that seen in Figure 1c for the submonthly timescale is evident with a broad anticyclonic circulation over southern Asia, a trough over Korea, a ridge in the western North Pacific, and a cyclonic circulation near 170°W, 20°N. It is also interesting to note that although they are similar, the ray path of alternating cyclonic and anticyclonic circulation centers on the submonthly timescale (in Figure 1c, for example) is somewhat south of the corresponding arc on the MJO timescale (in Figure 3a, for example). This is consistent with the modeling results of *Li and Nathan* [1994] who postulate that longer-timescale wave trains would penetrate farther into the midlatitudes than those on the shorter timescales.

## 4. Composite Results From Regressions

### Southeast Asia and Western Pacific Ocean

To illustrate the connection between the submonthly upper level circulation discussed above and the associated signature for midlatitude surface pressure surges on this timescale, Figure 3 is the regression between filtered 6- to 30-day OLR in the base area 5°N-5°S, 120°E-130°E and surface wind and SLP at all other grid points. This base area for OLR is close to the

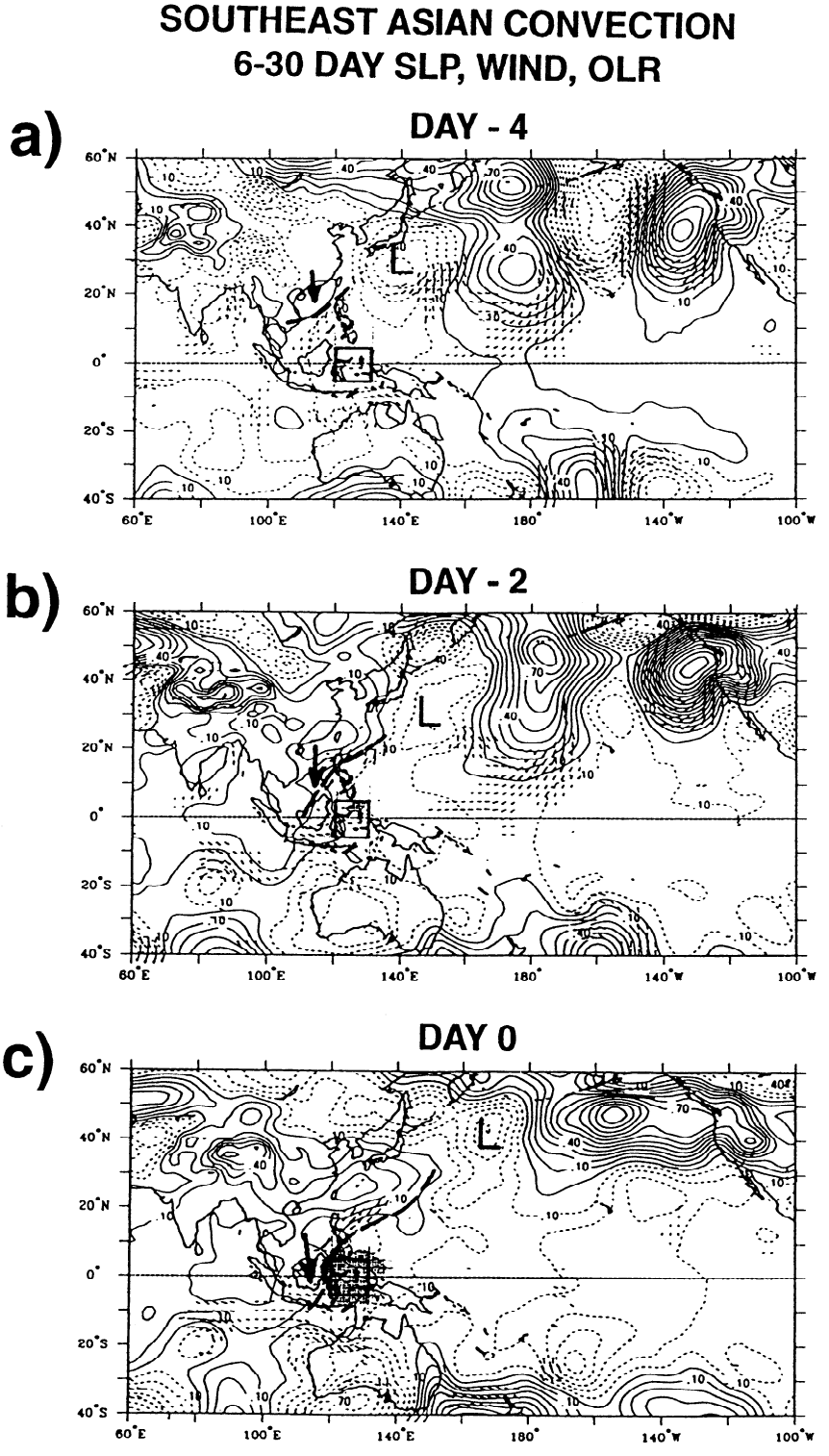


**Figure 3.** Composite OLR, sea level pressure (SLP), and surface vector wind anomalies in the 6- to 30-day band (submonthly timescale) during November-March 1985-1986 through 1992-1993 associated with area-averaged OLR in a base region over Southeast Asia (5°S-5°N, 120°E-130°E, indicated by box outline in plots): (a) circulation leading the peak in convection (as represented by low OLR in the base region) by 4 days (day −4); (b) by 2 days (day −2); and (c) simultaneous relationship (day 0). "L" indicates position of low-pressure center discussed in text, dashed contours are negative SLP anomalies, solid contours are positive SLP anomalies, heavy dashed line denotes leading edge of pressure surge signal, thick arrow indicates direction of motion of main body of pressure surge. Contour interval is 0.1 mbar. OLR standard deviation is 16.4 W $m^{-2}$.

region considered during the winter MONEX period over Southeast Asia [*Global Atmospheric Research Program (GARP)*, 1976]. The evolution of the 850 mbar circulation associated with 6- to 30-day convection over this region was examined by *Kiladis et al.* [1994, Figure 5]. Four days before the peak of convection, low pressure is set up just south of Japan. This is associated with the upper trough that was noted to be part of the wave train linked to prior convection in the eastern Indian Ocean in Figure 1c. In synoptic terms, this can be thought of as an enhancement of the signal of baroclinic waves taking place over a 6- to 30-day period with upper troughs just to the west of the surface lows. Meanwhile, a pressure surge (with direction of surge indicated by arrow) leaves the eastern Asian coast headed south across the South China Sea in Figure 3a at day −4. Two days before the peak of convection (Figure 3b, day −2), this pressure surge has crossed the South China Sea and reached the equatorial tropics in association with an alterating series of high- and low-pressure centers across the North Pacific. This pressure surge contributes to a near-equatorial surface pressure gradient (higher pressure to the west of Borneo) with weak surface wind convergence (small westerly wind anomalies near Borneo in Figure 3b), leading up to the convective blowup seen at day 0 (Figure 3c). Comparing the 850 mbar evolution from *Kiladis et al.* [1994, Figure 5], there is a well-developed "cyclone pair" anomaly with more pronounced equatorial westerly wind anomalies than at the surface by day 0, suggesting substantial modification of the flow by surface friction. There is no discernible connection to pressure surges in the southern hemisphere in Figure 3. This is partly due to the fact that pressure surges are more prevalent in the winter hemisphere even though, as described below, pressure surges from the summer southern hemisphere do seem to play a role farther to the east. The results in Figure 3 confirm the conventional view of pressure surges from eastern Asia contributing to blowups of convection over the Southeast Asian region noted in synoptic timescale studies for the winter MONEX period [e.g., *Lau et al.*, 1983; *Lau and Chang*, 1987; *Chang and Chen*, 1992; *Lau and Wu*, 1996].

To illustrate the connections between submonthly timescale patterns and midlatitude pressure surges for the western Pacific region, we choose a base area for OLR in the TOGA COARE region in the western Pacific (5°N–5°S, 150°E–160°E). The composite sequence from the regressions for 6– to 30-day filtered SLP, wind, and OLR evolves as shown in Figure 4, which can be compared with that for 850 mbar in Figure 6 of *Kiladis et al.* [1994]. Four days before the peak of convection in the western tropical Pacific the upper trough over eastern Asia (not shown) is somewhat farther east than in Figure 2 (consistent with an eastward translation of the midlatitude wave train noted earlier) and is associated with a surface low just east of Japan in Figure 4a. In conjunction with this surface low a pressure surge moves off the east coast of Asia with a southeastward trajectory, while a pressure surge is moving equatorward over eastern Australia in conjunction with a surface low in the southwestern Pacific (Figure 4a) and corresponding upper level trough off eastern Australia (not shown). Two days before the peak of convection in the western Pacific (Figure 4b) an upper trough in Figure 5a near Japan and a weak upper trough near New Zealand are associated with the pressure surges from either hemisphere in Figure 4b. There is also a downstream upper level wave train across the North Pacific in Figure 5a that roughly resembles the pattern in Figure 1c except that the wave train is shifted somewhat farther east. The pressure surges in Figure 4b contribute to a near-equatorial surface pressure gradient (higher pressure west of Papua New Guinea) with weak westerly winds and surface convergence in the western equatorial Pacific. This is followed two days later (Figure 4c) with a convective blowup in the TOGA COARE region in the western equatorial Pacific and westerly anomalies along the equator embedded within the convective region. As in the case from Figure 3, the 850 mbar flow from *Kiladis et al.* [1994] shows a much more developed cyclone pair anomaly and stronger westerlies than the surface flow, which actually has a substantial cross-equatorial flow in Figure 4. During the sequence in Figure 4 the midlatitude surface pressure centers translate east in association with the upper level wave train in Figure 5. This nearly equivalent barotropic structure is typical of perturbations advected within the Asian jet region on this timescale, as opposed to the more baroclinic structures seen on the synoptic timescale of less than 6 days. The upper level pattern seen in Figure 5 is rather different than the pattern associated with convective events in the Indian Ocean. Outflow from the convection in the western Pacific in Figure 5a is associated with an anomalously strong Asian jet east of the longitude of the convection, rather than at the same longitude as in Figure 1. This wave train in the northern hemisphere translates slowly to the east by day +2 in Figure 5c.

The MJO timescale midlatitude pattern associated with regional-scale convective blowups in the COARE region is shown in Figure 2b. The filtered 30– to 70-day 200 mbar streamfunction at all grid points is regressed against OLR in the western Pacific base region 15°S–5°N, 140°E–160°E. As noted for the Indian Ocean region there are also some similar elements in the MJO timescale and the submonthly timescale response in the western Pacific region (e.g., Figure 5c at day +2 for the submonthly timescale). These include a trough east of Japan, a wave train to the east arcing back into the tropics, and symmetric features south of the equator in the central Pacific. However, this wave train in Figure 5c for the submonthly timescale is shifted somewhat farther south and west compared to the MJO timescale in Figure 2b (varying the size of the base area for OLR does not significantly change the results). GCM experiments with specified diabatic heating anomalies corresponding to convective activity in the eastern Indian and western Pacific show steady state responses similar to those in Figure 2 for the MJO timescale [*Branstator*, 1990; *Meehl et al.*, 1993].

These results indicate that conditions in the midlatitudes can contribute to pressure surges from each hemisphere that reach the equatorial tropics. Comparing Figures 3 and 4, there are two types of composite pressure surges from Asia that have different trajectories. One type heads straight south across the South China Sea and is associated with convective blowups over Southeast Asia in the winter MONEX region. The other type tracks more to the southeast passing north of the Philippines and is associated with convection in the western equatorial Pacific. There is observational evidence for these two different types of pressure surges on the synoptic timescale over eastern Asia [*Wu and Chan*, 1995] and on the interannual timescale [*Lau et al.*, 1983]. There also appears to be little evidence in the canonical composites for interaction with the southern hemisphere midlatitudes for the Southeast Asian convective events. Yet southern hemisphere pressure surges appear to play more of a role in conjunction with surges from the northern hemisphere in western Pacific events.

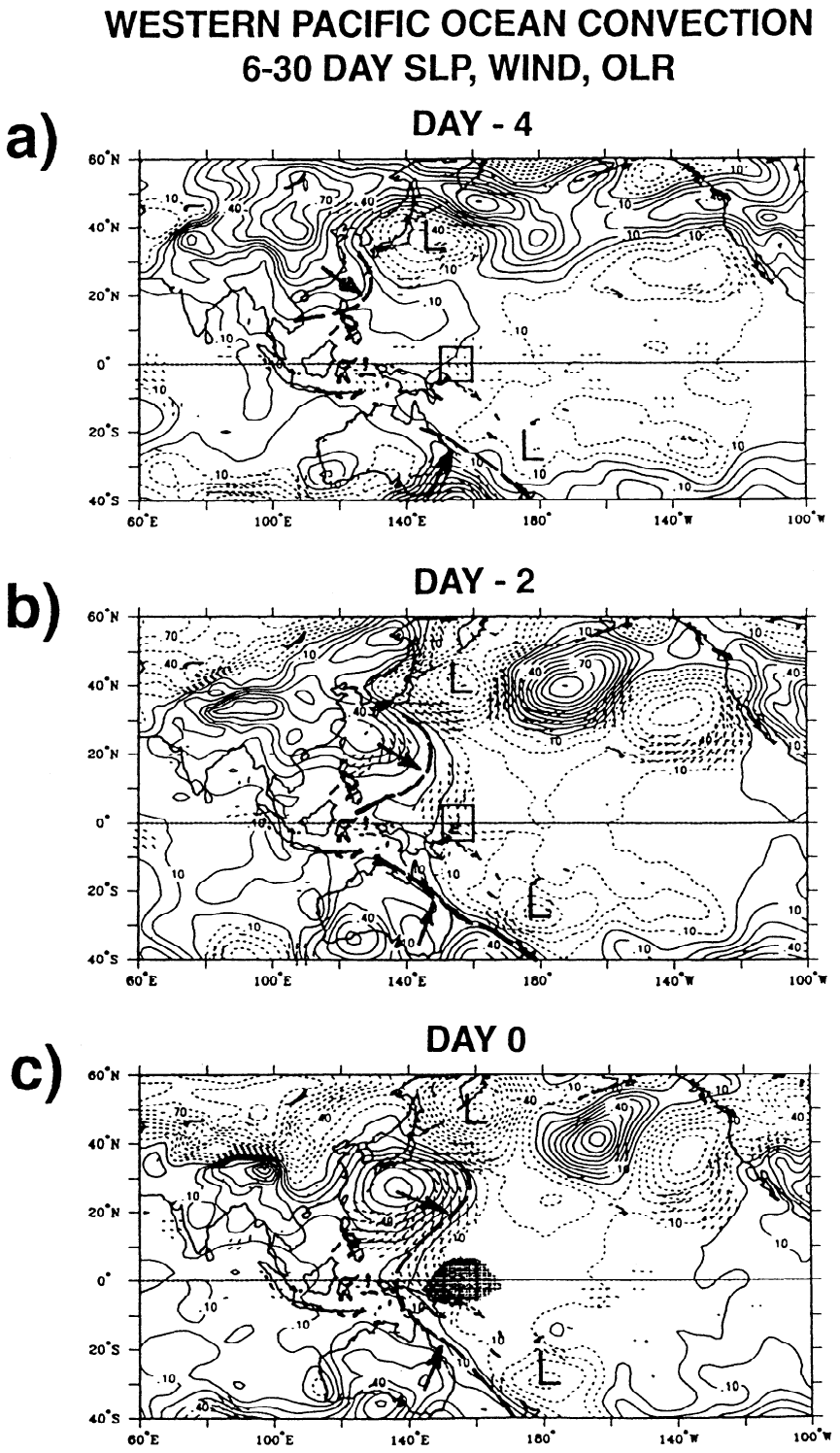


**Figure 4.** As in Figure 3 except for area-averaged OLR in a base region over the western equatorial Pacific Ocean (5°S-5°N, 150°E-160°E, indicated by box outline in plots). OLR standard deviation is 14.4 W $m^{-2}$.

## 5. December 1992 Case Study

Having reviewed canonical relationships between the large-scale aspects of surface and upper level circulations associated with the subseasonal eastward progression of regional-scale convection from the Indian Ocean to the western Pacific, we now examine in more detail features involved with the December 1992 period during TOGA COARE. The evolution of convective activity that took place during this period involved the eastward transition of an envelope of regional-scale convection from the Indian Ocean to the western Pacific [*Gutzler et al.*, 1994; *Lukas et al.*, 1995; *McBride et al.*, 1995; *Velden and Young*, 1994; *Lau et al.*, 1996; *Lin and Johnson*, 1996]. Figure 6 shows a Hovmuller diagram of the western Pacific OLR and equatorial 850 mbar zonal wind evolution during the TOGA

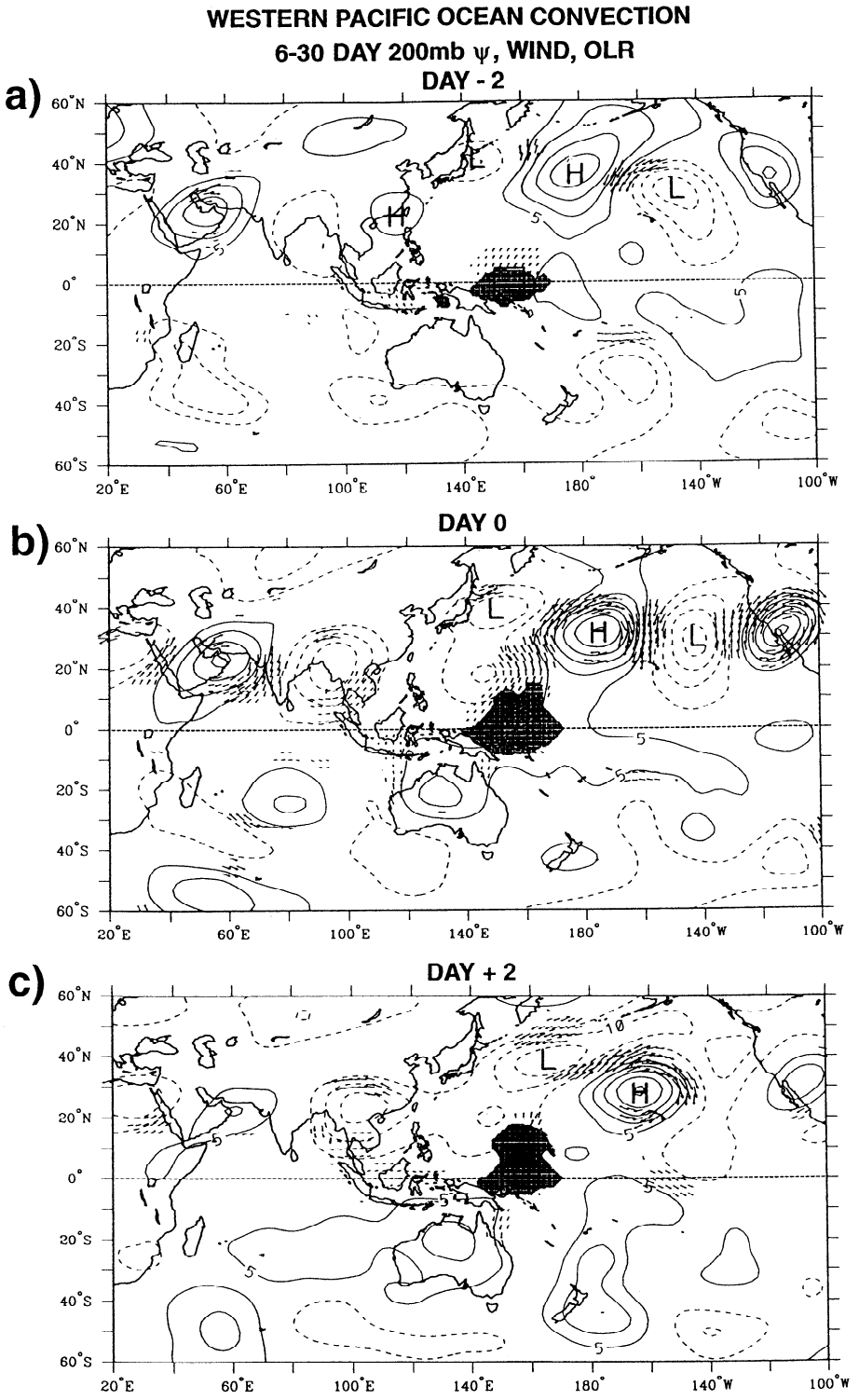


**Figure 5.** As in Figure 1 except for area-averaged OLR in a base region in the western equatorial Pacific Ocean (5°S-5°N, 150°E-160°E, indicated by box outline in plots): (a) day −2, (b) day 0, (c) day +2.

COARE period from November 10 to January 15. Equatorial westerlies are, in general, embedded within and to the west of the most active convection, which translates eastward through December at a speed typical of the MJO. This relationship, along with the surface pressure rises to the west of the convective envelope (not shown), is consistent with the signal seen in the composites shown by *Kiladis et al.* [1994]. Over the eastern Pacific, much of the westward propagation of the zonal wind signals evident in Figure 6 is associated with equatorial Rossby waves, as documented by *Kiladis and Wheeler* [1995].

We now examine the vertical structure of the winds in the western Pacific region to look for consistency with the results already presented for surface and upper level circulations and relate these to results previously presented by *Kiladis et al.*

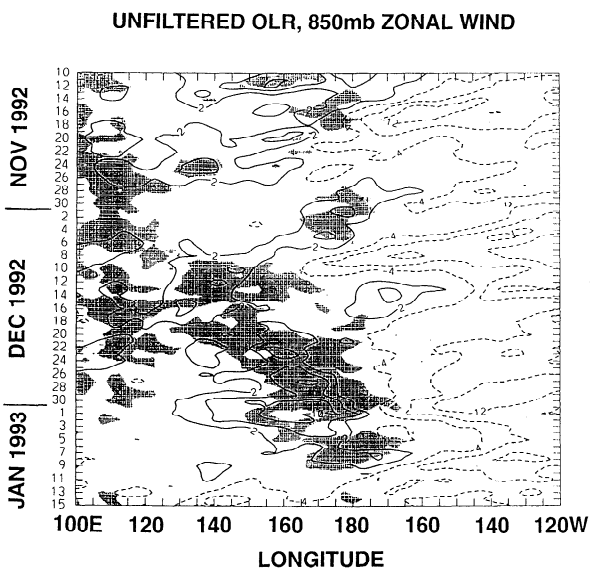


**Figure 6.** Hovmüller plot from 100°E to 120°W and from November 10, 1992, to January 15, 1993, of unfiltered OLR and 850 zonal wind averaged between 2.5°N and 2.5°S. OLR values less than 190 W $m^{-2}$ are shaded, and zonal winds of greater than 2 m $s^{-1}$ are shown by solid contours and less than $-4$ m $s^{-1}$ are shown by dashed contours, with an interval of 2 m $s^{-1}$.

[1994]. During TOGA COARE, four island-based and two ship-based portable weather stations (integrated sounding systems or ISS) were deployed in the equatorial western Pacific. The ISS units included surface observations, a lower tropospheric wind profiler, and omegasonde capability in addition to other functions [*Parsons et al.*, 1993]. In Figure 7 we show time-height plots of a blend of the omegasonde and profiler data. These data were input to the operational data assimilation stream and contributed to higher-quality analyses in this region. For comparison we also show time series from nearby grid points from the NMC analyses. Sampling, averaging, and the blending procedure are described by *Gutzler et al.* [1994].

Figure 7a shows the time-height plot of zonal wind from Kapingamarangi for a period in December 1992. Westerlies are seen to appear near the surface (i.e., near 998 mbar or about 90 m above the surface since this is the first level that the profiler obtains) in mid-December and continue into January. Westerly maxima occur above about 850 mbar up to around 600 mbar. There is a marked intensification of the easterlies aloft (near 100 mbar) with maximum values in excess of 35 m $s^{-1}$. The comparable product at a nearby grid point from the NMC analyses is shown in Figure 7b. Sustained westerlies near the surface become established around December 12 and continue unabated through the beginning of January with periods of winds near the surface greater than 5 m $s^{-1}$ for several days in late December and early January. Maximum westerly winds occur near 700 mbar, peaking in late December and early January. Easterlies aloft are also seen to intensify as the westerlies at the surface become established.

Farther west at Kavieng (3°S, 151°E, Figure 7c), the westerlies at the surface are stronger than at Kapingamarangi in Figure 7a. Westerlies greater than 5 m $s^{-1}$ occur frequently after mid-December. The maximum westerly winds occur above the surface between about 850 and 600 mbar as at Kapingamarangi. Easterlies aloft also intensify as the event develops. Comparing the ISS winds to the NMC analyses in Figure 7d, qualitative features are consistent between the two. However, as at Kapingamarangi, the analyzed westerlies near the surface are stronger than the observations, and the westerly wind maxima are closer to the surface. This indicates a bias in the operational analysis procedure, since there is generally quite good agreement between low-level winds from the ISS profilers and colocated radiosondes [*Riddle et al.*, 1996]. We note that the periods of very deep westerlies (above about 400 mbar) only occur for several days in early January. For most of the period, extensive westerly winds occur below 400 mbar. Thus the timescale of variations in the very deep westerlies is of the order of days (e.g., Figure 5b), and the MJO timescale (as represented in Figure 2b, for example) is characterized by easterly anomaly winds in the equatorial western Pacific in the upper troposphere (e.g., 200 mbar), while surface winds are westerly (e.g., Figure 4c). Thus the ISS soundings and grid point data from the operational analyses are consistent with the composite results of *Kiladis et al.* [1994] as well as with the results presented in Figures 2 and 5.

We next present a selection of representative quantities identified with the eastward movement of regional-scale convection shown in Figure 6 based on results presented above for the composite cross correlations. However, the relationships illustrated clearly in the composites are taking place in a case study setting amid convection and circulation features elsewhere in the tropics and midlatitudes that make interpretation of one particular set of processes challenging.

In Figure 8a the 6- to 30-day filtered 200 mbar streamfunction and OLR on December 11 show conditions coincident with convective activity that had been taking place near 100°E (Figure 6) in the Indian Ocean in the first part of December 1992. There is also convective activity occurring elsewhere in the tropics, but the midlatitude response over Asia and the Pacific appears to be associated most closely with the convective activity taking place in the Indian Ocean as seen in Figure 6. There is an anticyclonic circulation over southern Asia, a cyclonic circulation or trough over the east coast of Asia, an anticyclonic circulation over the western Pacific east of Japan, and a cyclonic circulation to the east near 150°W associated with a blowup of convection in the ITCZ just to the east near 140°W. This pattern resembles some aspects of the day +2 composite associated with convection in the eastern Indian Ocean in Figure 1c, most notably in connection with the wave train of anomalies extending eastward from the anticyclone to the north of the Bay of Bengal, and east Pacific ITCZ convection to the east of the upper trough located at about 160°W.

Figure 8b shows the 6- to 30-day filtered 850 mbar streamfunction and OLR one day later on December 12. In association with the ITCZ convection still in evidence near 140°W, a pair of cyclonic perturbations, one on either side of the equator, has formed immediately to the west with consequent equatorial westerlies and convection. A pair of weak anticyclones is also evident just to the west of the two lows. This resembles the lower tropospheric equatorial Rossby wave structure described by *Kiladis and Wheeler* [1995]. The surface pressure tendency map from the ECMWF analyses for December 14 in Figure 8c shows the consequent evolution of features at the surface in association with the upper level features a couple of days earlier shown in Figures 8a and 8b. In association with the trough over the eastern Asian coast in Figure 8a, as well as a similar trough for the 30- to 70-day filtered data during this

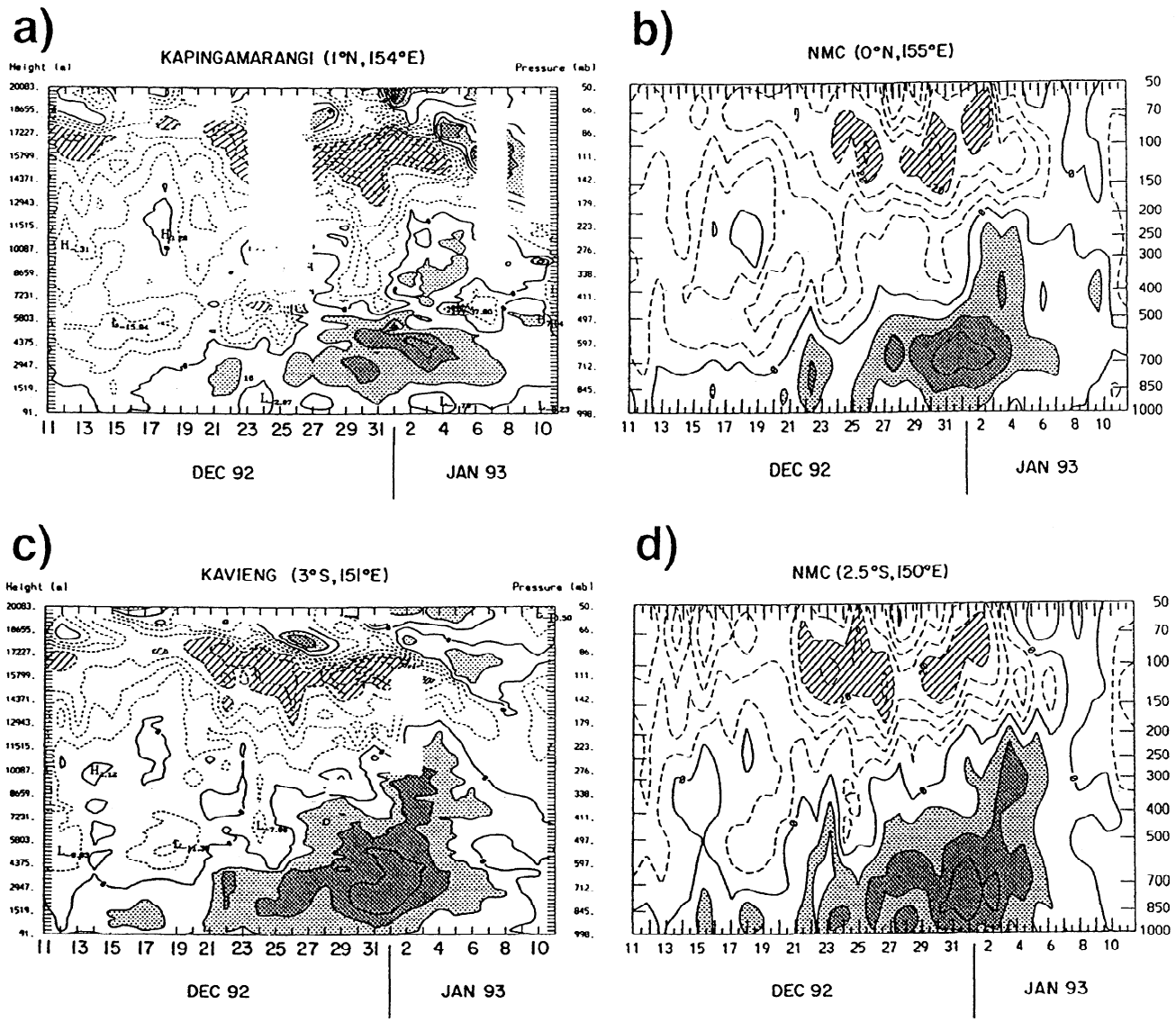


**Figure 7.** (a) Integrated sounding systems (ISS) zonal winds from Kapingamarangi for the December 1992 event. (b) National Meteorological Center (NMC) analyzed zonal winds at a grid point near Kapingamarangi for the December 1992 event. (c) ISS zonal winds from Kavieng for the December 1992 event. (d) NMC analyzed zonal winds at a grid point near Kavieng for the December 1992 event. Contour interval is 5 m $s^{-1}$. Missing data are left blank. Light stippling indicates westerlies greater than 5 m $s^{-1}$, dark stippling westerlies greater than 10 m $s^{-1}$, and hatching highlights easterlies greater than 20 m $s^{-1}$.

time period (not shown) that resembles some aspects of Figure 5a, surface pressures are falling east of Japan and a pressure surge has formed over eastern Asia (positive values indicating pressure rises in Figure 8c). This surge subsequently moves rapidly southward over the next two days (not shown), with no comparable surge from the southern hemisphere. It contributes to rising pressures over Southeast Asia and a subsequent convective outbreak in that region (Figure 6). This type of southward moving pressure surge resembles those termed "northerly surges" by *Wu and Chan* [1995]. They also correspond to the composite results in Figure 3 that show pressure surges from Asia during this stage moving southward associated with subsequent convection in the Southeast Asian region with little contribution from the southern hemisphere. This possible role of northerly pressure surges from Asia in this region was also noted by *Weickmann and Khalsa* [1990].

As convection increases over Southeast Asia in mid-December (Figure 6), the 6- to 30-day filtered 200 mbar streamfunction in Figure 9a during this period (December 18) indicates an anticyclonic circulation over the eastern Asian coast, a cyclonic circulation just east of Japan with a wave train arcing back toward the tropics to the east. In the southern hemisphere a cyclonic circulation is established east of Australia. The 6- to 30-day filtered 850 mbar data two days later on December 20 (Figure 9b) shows evidence of anticyclonic circulations (pressure surge signatures) near Japan and just east of Australia associated with the upper level troughs east of Japan and Australia that were in evidence two days earlier in Figure 9a. The equatorial Rossby wave signature noted in Figure 8b has weakened and moved westward to near the dateline, as noted in the mean behavior of composites shown by *Kiladis et al.* [1994]. The surface pressure tendency map for

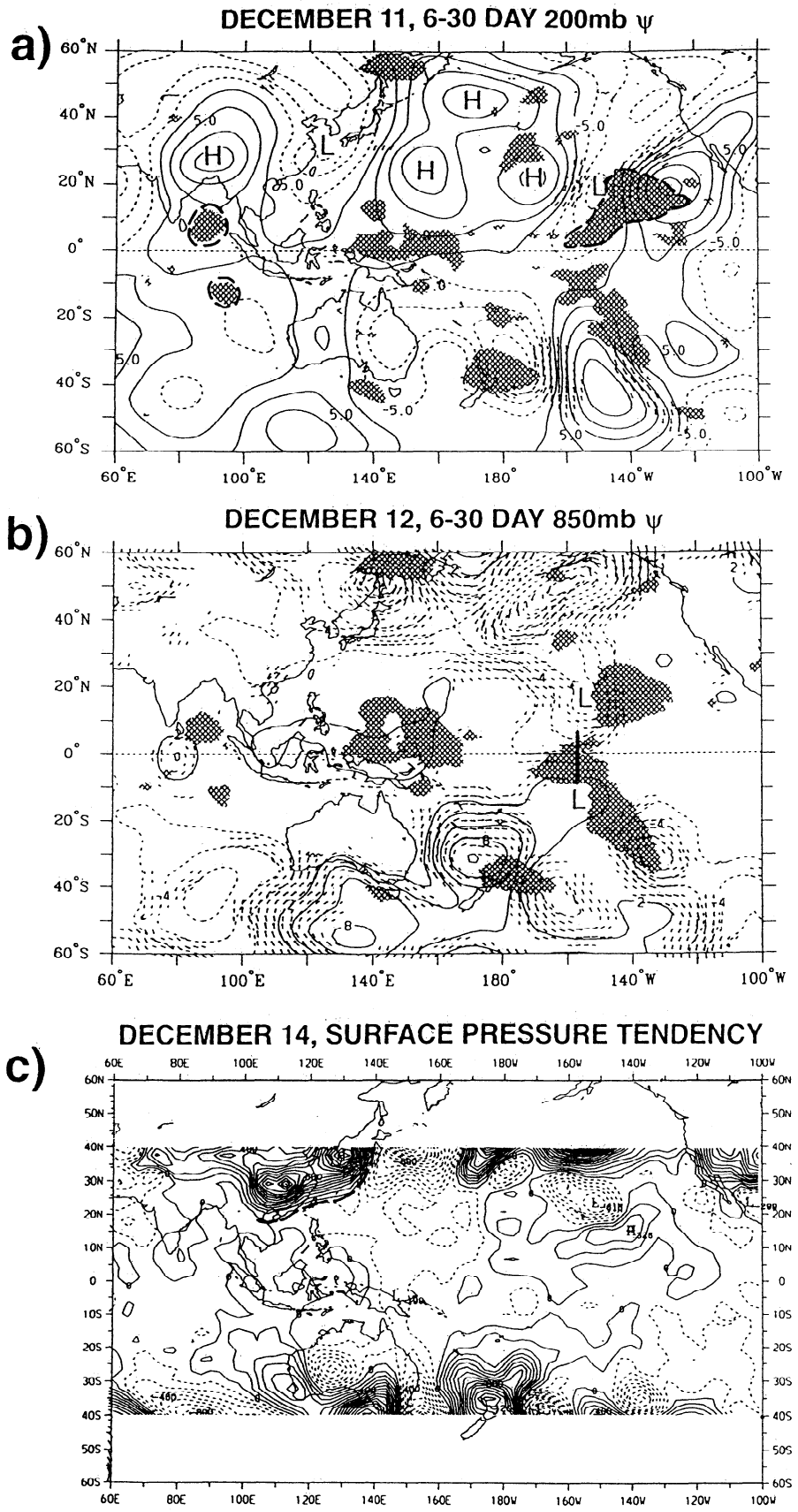


**Figure 8.** (a) December 11, 6- to 30-day filtered 200 mbar streamfunction contours and similarly filtered OLR (hatching); key areas of low OLR indicative of convective blowups discussed in text are outlined by thick dashed line. OLR values less than $-25$ W m$^{-2}$ are shaded. (b) December 12, 6- to 30-day filtered 850 mbar streamfunction contours and OLR (hatching); (c) December 14 surface pressure tendency (40°S-40°N only); positive values are solid contours indicating rising pressure. Approximate position of leading edge of pressure surge indicated by thick dashed lines. Contour interval is 1 mbar. For plot of total unfiltered equatorial convection, refer to Figure 6.

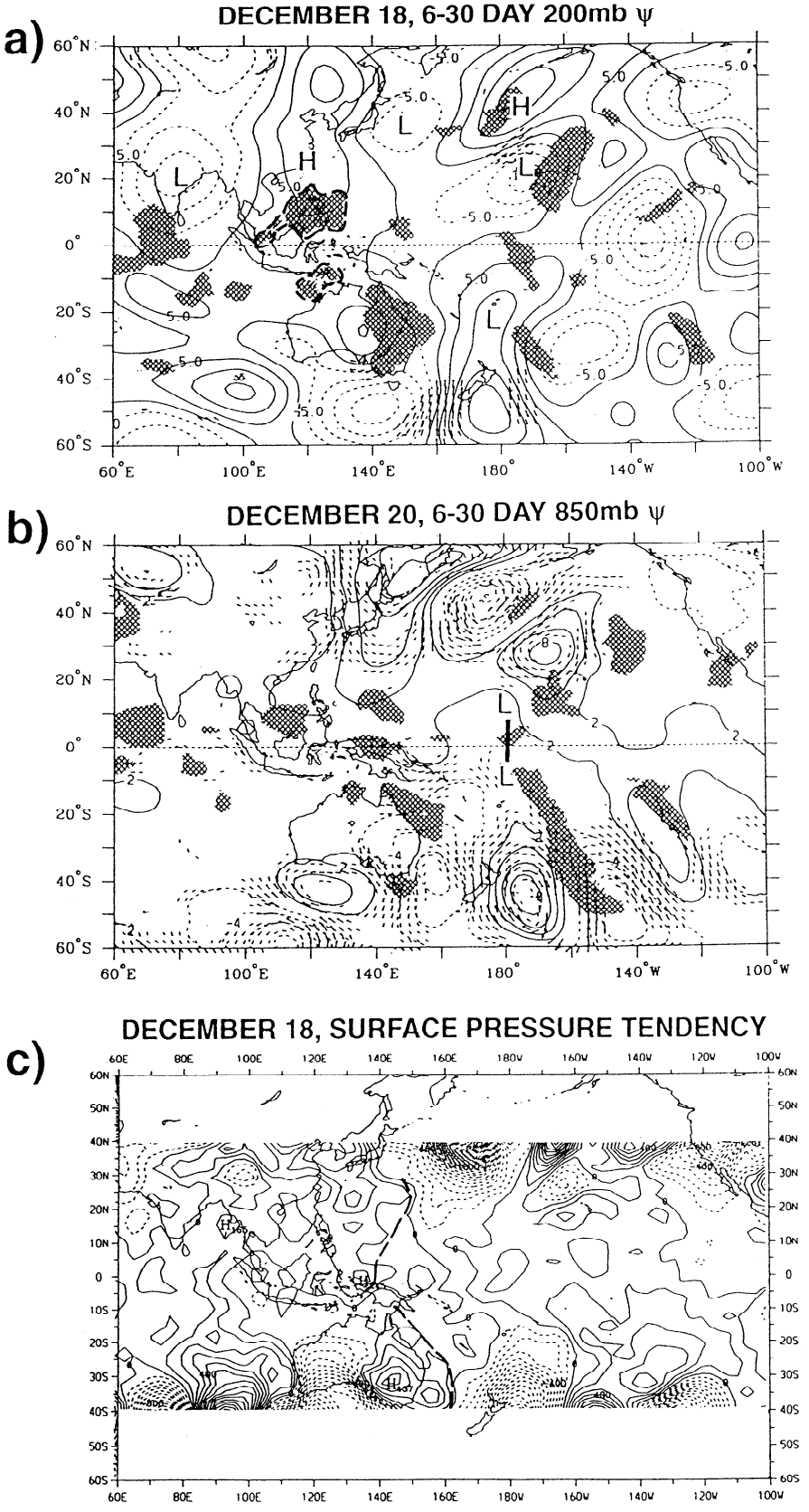


**Figure 9.** Examples for the December 1992 case study of features associated with total convective activity in the Southeast Asian region as shown in Figure 6. Filtered data do not depict all aspects of convection. For plot of total equatorial convection, refer to Figure 6. (a) December 18, 6- to 30-day filtered 200 mbar streamfunction contours and OLR (hatching); key areas of low OLR indicative of convective blowups discussed in text are outlined by thick dashed line. OLR values less than $-25$ W m$^{-2}$ are shaded. (b) December 20, 6- to 30-day filtered 850 mbar streamfunction contours and OLR (hatching); (c) December 18 surface pressure tendency (40°S-40°N only); positive values are solid contours indicating rising pressure. Approximate position of leading edges of pressure surges indicated by thick dashed lines. Contour interval is 1 mbar.

December 18 (Figure 9c), the same day as that in Figure 9a, shows pressure rises of several millibars east of Asia and near the east coast of Australia in association with the pressure surge signature noted in Figure 9b. The pressure surge off the east coast of Asia formed two days earlier over eastern Asia and moved southeastward, and the one over eastern Australia is moving northeastward after forming two days earlier over South Australia. Evidence that pressure surges from both hemispheres could contribute to near-equatorial pressure gradients and subsequent convection in the western equatorial Pacific was shown in the composites in Figure 4. For this period in December, these pressure surges are combining to raise surface pressure in the equatorial region near and to the west of Papua New Guinea, and to produce a west-east near-equatorial pressure gradient conducive to surface wind convergence as shown, for example, by *Chu* [1988] and *Lau et al.* [1995]. These conditions are occurring just prior to the shift of convection into the western equatorial Pacific around December 20 (Figure 6).

By December 25, convection has become established in the COARE region in the western Pacific (Figure 6) in association with the 30- to 70-day filtered 200 mbar streamfunction pattern shown in Figure 10a. There are anticyclonic circulations just to the north and south of the major mass of convective activity, with wave trains in either hemisphere that resemble some aspects of the 30- to 70-day filtered composite pattern in Figure 2b. The anticyclonic circulation in the Gulf of Alaska in Figure 2b is somewhat farther north in Figure 10a, and there is a secondary cyclonic circulation near New Zealand in the latter figure. Yet, the general features of the 200 mbar pattern in the composite in Figure 2b are similar to those in Figure 10a. These include a cyclonic circulation east of Japan, and twin cyclonic circulations on either side of the equator in the eastern Pacific that produce upper level equatorial westerlies.

On December 28 the 6- to 30-day filtered 200 mbar streamfunction map (Figure 10b) shows a wave train in the northern hemisphere with a cyclonic circulation near 160°E to the east of Japan and a wave train arcing back toward the tropics and crossing the equator in the eastern Pacific in association with the 30- to 70-day timescale 200 mbar equatorial westerlies noted there three days earlier in Figure 10a. The pattern in Figure 10b resembles that for the similar composite quantity in Figure 5c at day +2 for convection in the western Pacific. Concurrent with this wave activity and the associated convective blowup south of Baja California, equatorial Rossby waves can form in that region and move westward in the following days (not shown). Pressure surge activity continues in late December and is illustrated by the December 30 surface pressure tendency map in Figure 10c. Two pressure surges in either hemisphere are traveling equatorward (note pressure rises east of Japan and east of Australia), raising surface pressures over Indonesia and contributing to the surges in equatorial westerlies in the western Pacific (Figure 6). *Compo et al.* [1995] have noted pressure surge activity such as this over eastern Asia in the period following the major shift of convection from Asia to the central Pacific.

## 6. Discussion

On the basis of the results presented here and in earlier studies, we formulate a schematic diagram in Figure 11 to summarize an idealized eastward evolution of regional-scale tropical convection, tropical-midlatitude interaction, downstream development, and subsequent convective blowups in the TOGA COARE region in the western Pacific associated with westerly wind burst events during northern winter. Of course, the real system contains considerable noise and other possible outcomes. Additionally, for some of the features in Figure 11 we have shown only qualitative linkages in the present study. We will use this scenario as a framework within which to explore in more detail and to quantify various aspects of the interactions depicted in Figure 11.

We start with the "MJO envelope" of convection (hatched area, the ensemble of convective events on various timescales in that region, also termed a "super cloud cluster" by *Lau et al.* [1989]) in the Indian Ocean in Figure 11a. Associated with this regional-scale convective activity is a well-developed upper tropospheric wave train on the MJO timescale arcing into the northern hemisphere and a less well-developed wave train in the southern hemisphere (H and L enclosed in ellipses in Figure 11a). As a component of the MJO envelope of convection, submonthly timescale convection in the eastern Indian Ocean is associated with a similar pattern of midlatitude circulation and downstream blowups of convection in the eastern Pacific ITCZ as well as with connections to western North America. Intrusions of 6- to 30-day timescale vorticity into the tropics by the midlatitude wave train arcing into the eastern Pacific can initiate equatorial Rossby waves (noted in Figure 11a by the L enclosed by dashed circles in the equatorial eastern Pacific on either side of the equator) that move toward the west at about 7 m $s^{-1}$. The upper trough over eastern Asia, as part of the midlatitude wave train on the MJO and submonthly timescales, is associated with surface cyclones near the eastern Asian coast that form there and move east. Pressure surges to the west and south of these developing baroclinic waves then head south across the South China Sea into Southeast Asia to contribute to near-equatorial surface pressure gradients and convective activity there. Major upper level wind anomalies near 200 mbar are denoted by the thick solid arrows in Figure 11a, with mostly easterly wind anomalies extending from Southeast Asia across Africa and the Atlantic to the eastern Pacific [*Weickmann et al.*, 1996, Figure 2a].

As the MJO envelope of convection moves eastward, it crosses Southeast Asia in Figure 11b. Pressure surges mentioned in Figure 11a have set up near-equatorial surface pressure gradients that contribute to convection in this region as denoted in Figure 11b. The midlatitude wave trains in either hemisphere have translated somewhat to the east associated with a similar eastward shift of near-equatorial convective activity. The trough over eastern Asia and the surface low off the eastern Asian coast are also farther east and are associated with pressure surges leaving the Asian continent with a southeastward trajectory. The upper low over eastern Australia is also associated with equatorward surface pressure surges. The equatorial Rossby waves set off by the intrusion of a midlatitude upper level trough into the tropics of the eastern Pacific in Figure 11a cross the dateline heading west. Upper level wind anomalies are mostly easterly across southern Asia and northern Australia but are weak over the eastern Pacific.

Figure 11c depicts the situation as convection blows up in the western Pacific TOGA COARE region. Near-equatorial surface pressure gradients set up by the pressure surges in Figure 11b contribute to surface convergence and the initiation of convection, while in some cases equatorial Rossby waves arriving from the east can modulate the eastern extent of that convection. With the development of convection in the western

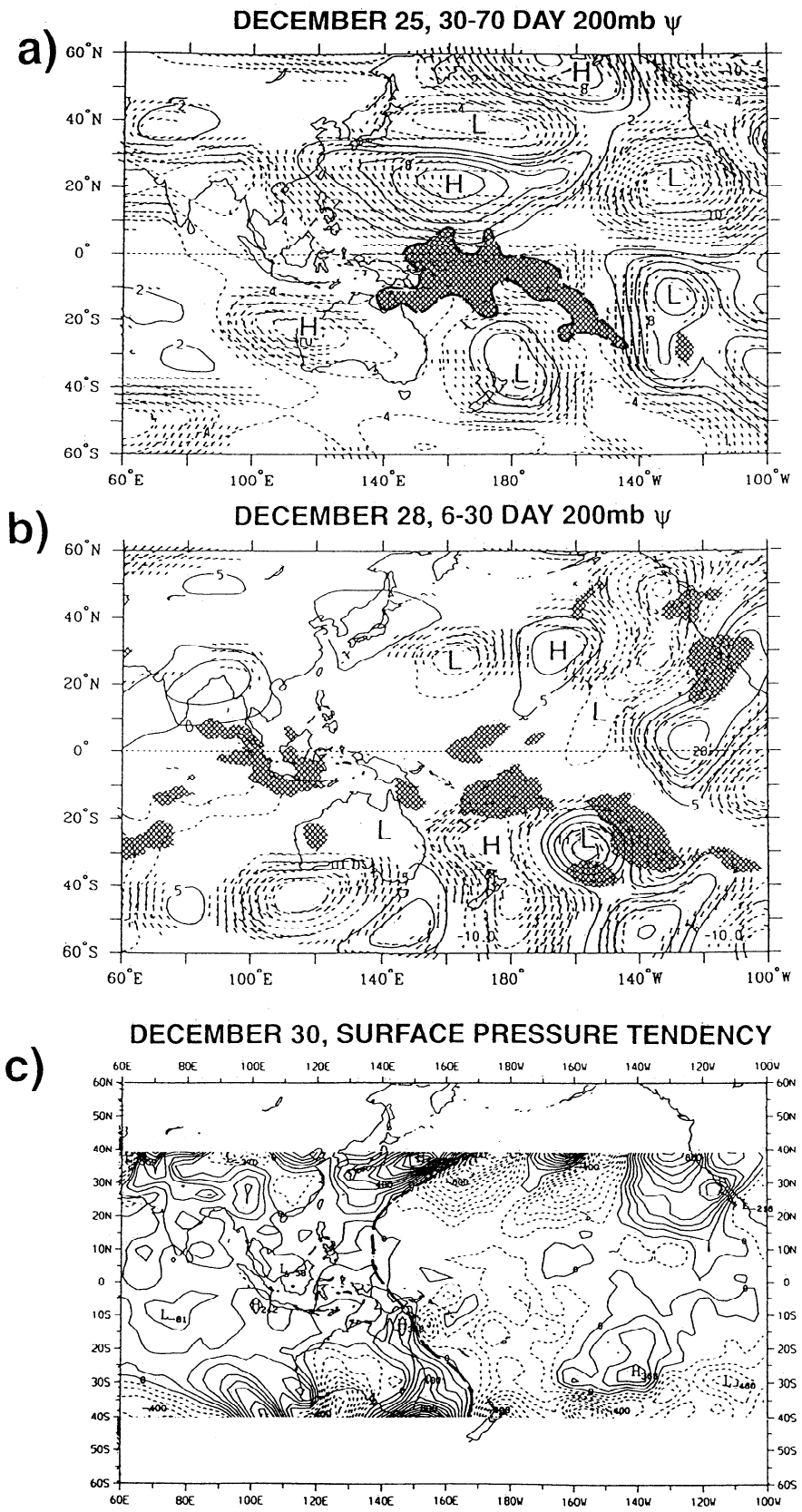


**Figure 10.** Examples for the December 1992 case study of features associated with convective activity in the western Pacific region as shown in Figure 6. Filtered data do not depict all aspects of convection. For plot of total equatorial convection, refer to Figure 6. (a) December 25, 30- to 70-day filtered 200 mbar streamfunction contours and OLR (hatching); key areas of low OLR indicative of convective blowups discussed in text are outlined by thick dashed line. OLR values less than $-25$ W m$^{-2}$ are shaded. (b) December 28, 6- to 30-day filtered 200 mbar streamfunction contours and OLR (hatching); (c) December 30 surface pressure tendency (40°S-40°N only); positive values are solid contours indicating rising pressure. Approximate position of leading edges of pressure surges indicated by thick dashed lines. Contour interval is 1 mbar.

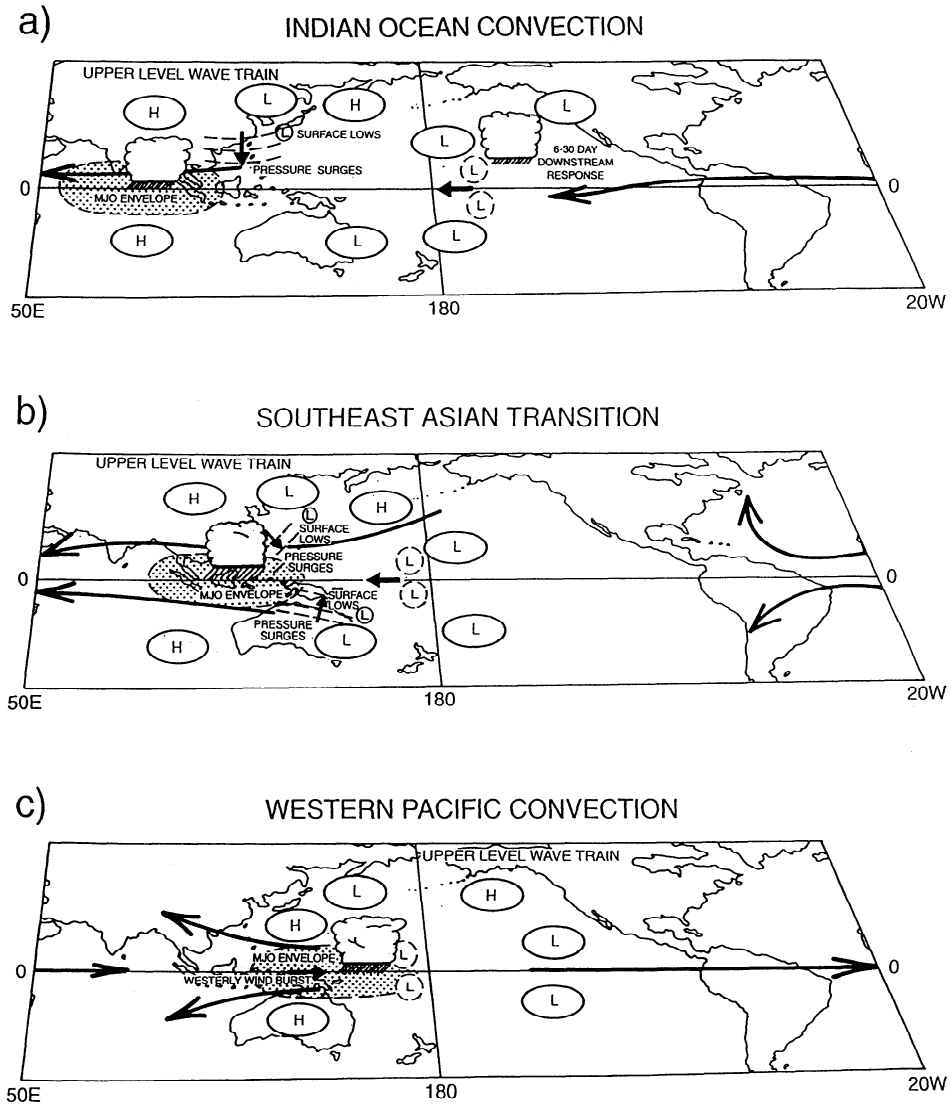


**Figure 11.** Schematic diagram of time and space scale interactions in the transition of a maximum of convective activity (stippled area) from (a) the eastern Indian Ocean, (b) across Southeast Asia, and (c) into the western equatorial Pacific. To give an example of the timescale, this transition occurred over about a 3-week period in the December 1992 case study described in the text. The H and L in ellipses indicate upper tropospheric circulation anomalies depicting major features of the 6–30 and MJO timescales. The L in dashed circles near equator denotes westward moving equatorial Rossby waves. L in solid circles indicates surface low-pressure areas. Thick solid arrows represent major features of anomalous upper tropospheric winds. Thin dashed lines near Australia and eastern Asia denote pressure surges.

Pacific, surface westerlies intensify. The upper level wave train has transitioned eastward, with upper level anticyclonic circulations to the north and south of the convective blowup. A wave train is arcing across the North Pacific along with a less well-developed one in the southern hemisphere. Upper level wind anomalies are now mostly easterly to the west of the MJO convective envelope, with westerlies extending from the eastern Pacific across the Atlantic and Africa to the western Indian Ocean [*Weickmann et al.*, 1996, Figure 2b]. As seen in the case study earlier, these upper level westerlies can enhance cross-equatorial wave propagation on shorter timescales.

Clearly there are numerous time and space scale interactions involved in the transition of convection from the Indian Ocean region to the TOGA COARE region in the western Pacific [see also *Weickmann and Khalsa*, 1990]. There is the interaction between the MJO and the submonthly timescales, with the MJO associated with an envelope of submonthly timescale convection. This envelope of convection sets up wave trains in either hemisphere, with the one in the northern (winter) hemisphere being stronger. Submonthly timescale convection in the eastern Indian Ocean has significant responses to the east that can include convective blowups in the eastern Pacific ITCZ, a trough formation over western North America and the initiation of equatorial Rossby waves that can travel westward from the region of the eastern Pacific ITCZ convective blowup. These equatorial Rossby waves, when present, can interact with subsequent near-equatorial pressure gradients caused by pressure surges from the midlatitudes (associated with the midlatitude wave train and eastern Asian trough set up by previous convection) and can contribute to the shift of

convection into the western Pacific and westerly wind burst events with their associated strong air-sea interactions [e.g., *Kindle and Phoebus*, 1995; *Lukas et al.*, 1995; *Zhang*, 1996]. The implications of this interaction in terms of the eastward extent of convection in the Pacific in relation to the base state sea surface temperatures (SSTs) in that region are explored by *Li and Wang* [1994] and *Kessler et al.* [1995].

## 7. Conclusions

We examine the eastward progression of convection from the Indian Ocean to the western Pacific to document large-scale aspects of reciprocal forcing-response between the tropics and the midlatitudes in the context of the submonthly or 6- to 30-day and MJO or 30- to 70-day timescales. This evolution can culminate with westerly wind burst events and strong air-sea interaction associated with regional-scale convective blowups in the TOGA COARE area in the western equatorial Pacific. These canonical evolutions are formed by using cross correlations between outgoing longwave radiation (OLR) and National Meteorological Center global analyses.

Tropical-midlatitude interactions are integral parts of this eastward progression as noted in previous studies. MJO timescale convection in the Indian Ocean is shown to be associated with a wave train downstream via the midlatitudes. Convection on the submonthly (6–30 days) timescale in the eastern Indian Ocean can be connected through a northern hemisphere wave train to convective blowups on that timescale in the ITCZ in the eastern Pacific. The intrusion of the midlatitude wave train into the tropical eastern Pacific can also be associated with the initiation of equatorial Rossby waves that move westward to interact with subsequent convective blowups in the western Pacific. The upper level trough over eastern Asia (part of the midlatitude wave train) is associated with pressure surges and subsequent convection over Southeast Asia. Such events near Borneo are preceded by pressure surges from the Asian continent with a southward trajectory. The composite events in the western equatorial Pacific TOGA COARE region farther to the east can be preceded by pressure surges from both the northern and the southern hemispheres as the midlatitude wave trains translate to the east along with the convective envelope in the tropics. These northern hemisphere surges have a more southeastward trajectory as they move from Asia toward the tropics compared to the southward surges in the winter MONEX region in Southeast Asia.

Omegasonde and profiler data from the integrated sounding systems (ISS) during TOGA COARE for the December 1992 westerly burst case study show strong vertical wind shear in the boundary layer (i.e., strongest winds occur just above the boundary layer), a sharply defined westerly maximum near 700 mbar, and an intensification of the upper level easterlies near 100 mbar. Westerlies are confined below about 300-400 mbar for most of the December 1992 period, with very deep westerlies (to 200 mbar) only occurring for about 6 days. Thus as suggested by the composite cross correlations, the very deep westerlies (through the depth of the troposphere) are a characteristic of the submonthly timescale [see also *Kiladis et al.*, 1994; *Kiladis and Wheeler*, 1995].

Surface pressure tendencies for the case study show that pressure surges from either hemisphere can play a role in the development of near-equatorial surface pressure gradients, subsequent surface convergence and a blowup of convection followed by strengthening surface westerlies. This sequence essentially confirms previous analyses of western Pacific westerly wind burst events but additionally points out the role of pressure surges from the southern hemisphere as noted in the cross correlations.

Alternating interactions between the tropics and midlatitudes suggested in previous studies are noted to be important here in the composites and case study, with the midlatitudes first forcing tropical convection via pressure surges and upper level wave energy, and the tropical convection then forcing the midlatitudes via midlatitude Rossby wave dispersion to set up extratropical circulation for subsequent pressure surges to the east. The submonthly Indian Ocean convective events provide an example of how processes at that timescale could subsequently affect North American weather via convective blowups in the eastern Pacific ITCZ.

The various time and space scale interactions for the eastward shift of convection are summarized schematically in terms of a scenario that is to be examined further in subsequent studies. Such studies presently under way include efforts to quantify further the relationships between the submonthly and the MJO timescales; to examine the role of the equatorial Rossby wave disturbances (associated with intrusions of upper level midlatitude Rossby wave activity into the tropical eastern Pacific) that can play a role in the subsequent western Pacific convective activity; to elucidate features of boundary layer wind shear and vertical wind structure in western Pacific westerly wind burst events; to analyze additional case studies to determine the degree to which we can generalize the results from the case study in the present paper; and to document further the role of midlatitude pressure surges in forcing tropical convection.

**Acknowledgments.** The authors acknowledge Grant Branstator for helpful comments and discussions. This research was supported in part by a TOGA COARE project grant through the National Science Foundation under grant ATM-9205914 as well as by the Office of Health and Environmental Research of the U.S. Department of Energy under its Carbon Dioxide Research Program. The National Center for Atmospheric Research is supported by the National Science Foundation.

## References

Branstator, G. W., Mechanisms affecting the midlatitude atmospheric response to equatorial heating anomalies, paper presented at TOGA International Scientific Conference, Honolulu, World Meteorol. Organ., Geneva, 1990.

Chang, C.-P., and J.-M. Chen, A statistical study of winter monsoon cold surges over the South China Sea and the large-scale equatorial divergence, *J. Meteorol. Soc. Jpn.*, *70*, 287–302, 1992.

Chen, T.-C., J.-M. Chen, J. Pfaendtner, and J. Susskind, The 12–24 day mode of global precipitation, *Mon. Weather Rev.*, *123*, 140–152, 1995.

Chu, P.-S., Extratropical forcing and the burst of equatorial westerlies in the western Pacific: A synoptic study, *J. Meteorol. Soc. Jpn.*, *66*, 549–564, 1988.

Compo, G. P., G. N. Kiladis, and P. J. Webster, Modulation of tropical-extratropical interaction by the Madden-Julian Oscillation, *WCRP-91 WMO/TD 717*, 147–151, World Meteorol. Organ., Geneva, 1995.

Davidson, N. E., J. L. McBride, and B. J. McAvaney, The onset of the Australian monsoon during winter-MONEX: Synoptic aspects, *Mon. Weather Rev.*, *111*, 496–516, 1983.

Ferranti, L., T. N. Palmer, F. Molteni, and E. Klinker, Tropical-extratropical interaction associated with the 30-60 day oscillation and its impact on medium and extended range prediction, *J. Atmos. Sci.*, *47*, 2177–2199, 1990.

Global Atmospheric Research Program (GARP), *The Monsoon Ex-*

*periment, GARP Publ. Ser. 18*, 124 pp., World Meteorol. Organ., Geneva, 1976.

Gutzler, D. S., G. N. Kiladis, G. A. Meehl, K. M. Weickmann, and M. Wheeler, The global climate of December 1992-February 1993, II, Large-scale variability across the tropical western Pacific during TOGA COARE, *J. Clim.*, *7*, 1606–1622, 1994.

Hartmann, D. L., M. L. Michelsen, and S. A. Klein, Seasonal variations of tropical intraseasonal oscillations: A 20-25 day oscillation in the western Pacific, *J. Atmos. Sci.*, *49*, 1277–1289, 1992.

Hendon, H. H., and B. Liebmann, Organization of convection within the Madden-Julian Oscillation, *J. Geophys. Res.*, *99*, 8073–8083, 1994.

Hoskins, B. J., and T. Ambrizzi, Rossby wave propagation on a realistic longitudinally varying flow, *J. Atmos. Sci.*, *50*, 1661–1671, 1993.

Hsu, H.-H., B. J. Hoskins, and F.-F. Jin, The 1985/86 intraseasonal oscillation and the role of the extratropics, *J. Atmos. Sci.*, *47*, 823–839, 1990.

Kessler, W. S., M. J. McPhaden, and K. M. Weickmann, Forcing of intraseasonal Kelvin waves in the equatorial Pacific, *J. Geophys. Res.*, *100*, 10613–10631, 1995.

Kiladis, G. N., and K. M. Weickmann, Circulation anomalies associated with tropical convection during northern winter, *Mon. Weather Rev.*, *120*, 1900–1923, 1992a.

Kiladis, G. N., and K. M. Weickmann, Extratropical forcing of tropical Pacific convection during northern winter, *Mon. Weather Rev.*, *120*, 1924–1938, 1992b.

Kiladis, G. N., and M. Wheeler, Horizontal and vertical structure of observed tropospheric equatorial Rossby waves, *J. Geophys. Res.*, *100*, 22,981–22,997, 1995.

Kiladis, G. N., G. A. Meehl, and K. M. Weickmann, Large-scale circulation associated with westerly wind bursts and deep convection over the western equatorial Pacific, *J. Geophys. Res.*, *99*, 18,527–18,544, 1994.

Kindle, J. C., and P. A. Phoebus, The ocean response to operational westerly wind bursts during the 1991-1992 El Nino, *J. Geophys. Res.*, *100*, 4893–4920, 1995.

Lau, K.-M., and C.-P. Chang, Planetary scale aspects of the winter monsoon and atmospheric teleconnections, in *Monsoon Meteorology*, edited by C.-P. Chang and T. N. Krishnamurti, pp. 161–202, Oxford Univ. Press, New York, 1987.

Lau, K.-M., and H.-T. Wu, Large scale dynamics associated with super cloud cluster organization over the tropical western Pacific, *J. Meteorol. Soc. Jpn.*, in press, 1996.

Lau, K.-M., C.-P. Chang, and P. H. Chan, Short-term planetary scale interactions over the tropics and midlatitudes, II, Winter-MONEX period, *Mon. Weather Rev.*, *111*, 1372–1388, 1983.

Lau, K.-M., L. Peng, C. H. Sui, and T. Nakazawa, Dynamics of super cloud clusters, westerly wind bursts, 30-60 day oscillations and ENSO: A unified view, *J. Meteorol. Soc. Jpn.*, *67*, 205–219, 1989.

Lau, K.-M., P. J. Sheu, S. Schubert, D. Ledvina, and H. Weng, Evolution of large scale circulation during TOGA-COARE: Model intercomparison and basic features, *J. Clim.*, in press, 1996.

Li, L., and T. R. Nathan, The global atmospheric response to low-frequency tropical forcing: Zonally averaged basic states, *J. Atmos. Sci.*, *51*, 3412–3426, 1994.

Li, T., and B. Wang, The influence of SST on the tropical intraseasonal oscillation: A numerical study, *Mon. Weather Rev.*, *122*, 2349–2362, 1994.

Lin, X., and R. H. Johnson, Kinematic and thermodynamic characteristics of the flow over the western Pacific warm pool during TOGA COARE, *J. Atmos. Sci.*, *53*, 695–715, 1996.

Livezey, R. E., and W. Y. Chen, Statistical field significance and its determination by Monte Carlo techniques, *Mon. Weather Rev.*, *111*, 46–59, 1983.

Love, G., Cross-equatorial influence of winter hemisphere subtropical cold surges, *Mon. Weather Rev.*, *113*, 1499–1509, 1985.

Lukas, R., P. J. Webster, M. Ji, and A. Leetma, The large-scale context for the TOGA Coupled Ocean-Atmosphere Response Experiment, *Meteorol. Atmos. Phys.*, *56*, 3–16, 1995.

Lyons, S. W., Planetary-scale aspects of outgoing longwave radiation and vorticity over the global tropics during winter, *Mon. Weather Rev.*, *109*, 1773–1787, 1981.

Madden, R., and P. Julian, Observations of the 40-50-day tropical oscillation—A review, *Mon. Weather Rev.*, *122*, 814–837, 1994.

Matsuno, T., Quasi-geostrophic motions in the equatorial area, *J. Meteorol. Soc. Jpn.*, *44*, 25–43, 1996.

McBride, J. L., N. E. Davidson, K. Puri, and G. C. Tyrell, The flow during TOGA COARE as diagnosed by the BMRC tropical analysis and prognosis system, *Mon. Weather Rev.*, *123*, 717–736, 1995.

McPhaden, J. J., F. Bahr, Y. Penhoat, E. Firing, S. P. Hayes, P. P. Niiler, P. L. Richardson, and J. M. Toole, The response of the western equatorial Pacific Ocean to westerly wind bursts during November 1989 to January 1990, *J. Geophys. Res.*, *97*, 14,298–14,303, 1992.

Meehl, G. A., Coupled land-ocean-atmosphere processes and South Asian monsoon variability, *Science*, *266*, 263–267, 1994.

Meehl, G. A., G. W. Branstator, and W. M. Washington, Tropical Pacific interannual variability and $CO_2$ climate change, *J. Clim.*, *6*, 42–63, 1993.

Murakami, T., Temporal variations of satellite-observed outgoing longwave radiation over the winter monsoon region, I, Long-period (15-30 day) oscillations, *Mon. Weather Rev.*, *108*, 408–426, 1980.

Numaguti, A., Characteristics of 4-to-20-day period disturbances observed in the equatorial Pacific during TOGA COARE IOP, *J. Meteorol. Soc. Jpn.*, *73*, 353–377, 1995.

Parsons, D., et al., The Integrated Sounding System: Description and preliminary observations from TOGA COARE, *Bull. Am. Meteorol. Soc.*, *75*, 553–567, 1993.

Riddle, A. C., W. M. Angevine, W. L. Ecklund, E. R. Miller, D. B. Parsons, D. A. Carter, and K. S. Gage, In situ and remotely sensed horizontal winds and temperature intercomparisons obtained using Integrated Sounding Systems during TOGA COARE, *Contr. Atmos. Phys.*, in press, 1996.

Schrage, J. M., and D. G. Vincent, Composite studies of the large-scale atmospheric state on 7-21 day timescales during active and inactive convection episodes, *WCRP-91 WMO/TD 717*, pp. 44–47, World Meteorol. Organ., Geneva, 1995.

Trenberth, K. E., and J. G. Olson, An evaluation and intercomparison of global analyses from the National Meteorological Center and the European Center for Medium Range Weather Forecasts, *Bull. Am. Meteorol. Soc.*, *69*, 1047–1057, 1988.

Velden, C. S., and J. A. Young, Satellite observations during TOGA COARE: Large-scale descriptive overview, *Mon. Weather Rev.*, *122*, 2426–2441, 1994.

Webster, P. J., and R. Lukas, TOGA COARE: The Coupled Ocean-Atmosphere Response Experiment, *Bull. Am. Meteorol. Soc.*, *73*, 1377–1416, 1992.

Weickmann, K. M., and S. J. S. Khalsa, The shift of convection from the Indian Ocean to the western Pacific Ocean during a 30-60 day oscillation, *Mon. Weather Rev.*, *118*, 964–978, 1990.

Weickmann, K. M., G. N. Kiladis, and P. Sardeshmukh, A composite intraseasonal atmospheric angular momentum budget during northern winter, *J. Atmos. Sci.*, in press, 1996.

Wu, M. C., and J. C. L. Chan, Surface features of winter monsoon surges over South China, *Mon. Weather Rev.*, *123*, 662–680, 1995.

Zhang, C., Atmospheric intraseasonal variability at the surface in the tropical western Pacific Ocean, *J. Atmos. Sci.*, *53*, 739–758, 1996.

G. P. Compo, Program in Atmospheric and Oceanic Sciences, University of Colorado, Boulder, CO 80302.

D. S. Gutzler, University of New Mexico, Albuquerque, NM 87106.

G. N. Kiladis and M. Wheeler, Aeronomy Laboratory, NOAA, Boulder, CO 80303.

K. M. Weickman, Climate Diagnostics Center, Boulder, CO 80303.

G. A. Meehl (corresponding author), National Center for Atmospheric Research, P. O. Box 3000, 1850 Table Mesa Drive, Boulder, CO 80307-3000.

(Received October 15, 1995; revised March 20, 1996;
accepted March 20, 1996.)